1985ApJ...291...32B

THE ASTROPHYSICAL JOURNAL, 291:32–44, 1985 April 1
© 1985. The American Astronomical Society. All rights reserved. Printed in U.S.A.

THE ORIENTATIONS OF THE ROTATION AXES OF RADIO GALAXIES. I. RADIO MORPHOLOGIES OF BRIGHT ELLIPTICAL GALAXIES

M. BIRKINSHAW
Mullard Radio Astronomy Observatory, University of Cambridge
AND
ROGER L. DAVIES
Kitt Peak National Observatory, National Optical Astronomy Observatories[1]
Received 1984 July 11; accepted 1984 October 19

ABSTRACT

The results of VLA observations of 47 bright elliptical galaxies from a sample of 54 galaxies for dynamical study are presented, and the structures of the extended sources are described. No evidence is found for a unique alignment of the radio axes and minor axes of the host galaxies. The distribution of misalignment angles is consistent with being uniform between 0° and 50°, with larger misalignments being significantly less likely. We found no significant correlations between the radio power or misalignment angle and any of the intrinsic kinematic parameters, in particular rotation velocity and central velocity dispersion.

Subject headings: galaxies: internal motions — galaxies: jets — galaxies: structure — radio sources: galaxies

I. INTRODUCTION

Radio "jet" structures many kiloparsecs in length are a common feature of extragalactic radio sources (e.g., Cygnus A, Perley, Dreher, and Cowan 1984; 3C 31, Burch 1977; M87, Biretta, Owen, and Hardee 1983), and are usually taken as tracers of the collimated flow of material emitted continuously or sporadically from some compact engine in a galaxy nucleus (Blandford and Rees 1974). The elongated jet features may be almost straight, as in NGC 6251 (Saunders *et al.* 1981), or curved through a large angle, as in 3C 388 (Burns and Christiansen 1980), and are known in some cases to originate with a VLBI jet which is already collimated on a scale of a few parsecs (e.g., NGC 6251, Readhead, Cohen, and Blandford 1978). The straightness of a jet, and the absence of discontinuities in its direction, reflect the persistence of the direction of emission of the beam of material from the generator: for NGC 6251, the jet curves over $\sim 10°$ in position angle over its length of ~ 200 kpc (Saunders *et al.* 1981), corresponding to a stability of orientation of the beam generator to less than about 10° over about 10^7 yr. Note, however, that the parsec-scale jet and the kiloparsec-scale jet are misaligned by about 10° in this galaxy, so that there is bending of the jet on a scale of ~ 50 pc.

The mechanisms that trigger radio activity in galaxies and determine the direction of emission of a jet are unknown. However, once the central engine driving the radio source is in place in the nucleus of its host galaxy, only small accretion rates ($\sim 10\ M_\odot\ \mathrm{yr}^{-1}$) are required to fuel it, and it is surmised (e.g., Rees 1978) that the direction of the jets in radio galaxies is that of some preferred axis, presumably an axis of rotation, of the accreting engine. The relationship between this central engine and the host galaxy, and the origin of the material fueling it, are topics of considerable speculation. If the central engine was formed and fueled by material which originated in the host galaxy—for example, from mass lost during stellar evolution—then it might be expected that the rotation axis of the engine (and thus the radio axis) would align with the rotation axis of the stars. However, if the central object was formed in another galaxy which was later captured by the host, or if the fuel originates outside the host galaxy, then such an alignment would not be expected.

The determination of the rotation axes of elliptical galaxies cannot reliably be done from their stellar figures: the slow rotations and isophote twists observed in elliptical galaxies suggest that their figures may be triaxial, and hence that their projected minor axes may not be coincident with their rotation axes. We must, therefore, make velocity maps of radio elliptical galaxies in order to determine their rotation axes for comparison with the radio axes. As a first step, we present here radio maps of a sample of bright elliptical galaxies chosen so that good velocity mapping is possible. We aim to determine whether the radio axes are aligned with the rotation axes of the stars on kpc scales. Such an alignment would support strongly the hypothesis that the host galaxy determines the properties of the engine driving the radio source, and provides the fuel to power it. Lack of alignment would perhaps indicate that either the engine or the fuel, or both, originate outside the host galaxy.

This paper is concerned with the radio structures of the elliptical galaxies in a sample chosen so that good optical spectroscopy is possible. Later papers will deal with detailed stellar-dynamical maps of those galaxies with suitable radio structures, and the interpretation of the results in the context of the beam model. Section II of this paper discusses previous work intended to test the beam model through studies of morphological or dynamical data on the galaxies. In § III we present the sample of 54 galaxies studied here and their optical properties. Radio observations using the VLA have been made for all 47 of the galaxies in this sample for which good radio data were not previously available; these observations are detailed in § IV, and the radio structures of the detected galaxies are discussed in the Appendix. Section V then examines the relative orientations of the minor and radio axes of those 22 galaxies displaying extended radio emission, and identifies

[1] Operated by the Association of Universities for Research in Astronomy, Inc., under contract with the National Science Foundation.

© American Astronomical Society • Provided by the NASA Astrophysics Data System

1985ApJ...291...32B

the galaxies which are useful for later dynamical study. This dynamical study will be the subject of a later paper.

Throughout this paper we shall assume $H_0 = 50$ km s^{-1} Mpc^{-1} and $q_0 = 0$.

II. PREVIOUS STUDIES: THE GALAXY SAMPLE

Most previous studies of the relationship between the radio and dynamical axes of galaxies have assumed that the dynamical axis of a galaxy is the same as the minor axis of the stellar figure (as seen on deep plates), and then have examined the correlation between the minor and radio axes (see Guthrie 1979 and references therein; also Kapahi and Saikia 1982). This approach enables a large sample of galaxies to be studied quickly. However, the generally low rotation velocities and isophote twists of elliptical galaxies may indicate that they are not oblate but triaxial (Illingworth 1977; Binney 1978), so that the projected minor and dynamical axes may not be coincident.

The result of these earlier morphological studies of the alignment of the radio axes is that the minor axis is preferred over the major axis for association with the radio emission direction. This result is ambiguous: the trend for alignment exists, but the preference is small and many large misalignments are seen. Morphological complications intrinsic to elliptical galaxies complicate the issue: (1) The minor-axis position angles are determined at faint isophote levels, far away from the important nuclear regions. If the galaxies are triaxial, they may have twisted isophotes, so that the minor axis at small radii can be significantly misaligned with that measured at large radii. (2) The presence of faint dust lanes can bias the measurement of the position angle of the stellar component. (3) Many bright radio galaxies are almost round and are optically faint, so the position-angle determinations can be quite uncertain.

A direct study of the rotation axes of radio elliptical galaxies is appropriate, but few studies of the dynamics of radio elliptical galaxies have been made. For strong radio galaxies, the stellar component is usually faint; the stellar rotation axes have been measured for *no* radio galaxies with $P_{178} \gtrsim 2 \times 10^{25}$ W Hz^{-1} sr^{-1}. For nearby, and hence weaker, radio galaxies, stellar rotation curves have been measured, but the results are inconclusive, with significant misalignments between the radio and rotation axes in several cases, and good alignments in others. Simkin (1979) concluded that in 3C 33, 3C 98, and 3C 218 the minor axis of the figure, the rotation axis of the stars, and the axis of the radio source are well aligned, but the galaxies were found to be unusual in showing very large rotation velocities compared with normal ellipticals. On the other hand, Jenkins and Scheuer (1980) and Jenkins (1981) found substantial misalignments between the projected minor axes and the kinematic axes of seven weaker radio galaxies, and neither axis was found to align with the radio structure.

Thus it appears that powerful radio sources show alignments between their radio and dynamical axes, whereas less powerful sources do not. It is tempting to interpret this dichotomy in terms of different origins for the fuel powering the radio emission. In powerful radio galaxies, the radio emission could be fueled by material originating in the galaxy, whereas in the less powerful sources the fuel supply to the central engine might originate from an external source, and hence turn the rotation axis of the beam generator to an "unusual" orientation. Misalignments between the minor and dynamical axes of normal elliptical galaxies are rare (Schechter and Gunn 1979; Davies and Illingworth 1985; but see Williams 1981), although the sample studied is small. Jenkins (1981) rejected the infall hypothesis for triggering radio activity and concluded that the anomalous stellar kinematic properties of radio elliptical galaxies is directly related to the origin of their radio activity. He suggested that formation by mergers could account for the misalignment of their central engines with their kinematic and geometric axes.

In order to examine this question more closely, we have chosen to study the dynamics of a large sample of nearby galaxies. The direct determination of dynamical axes is limited by the large amount of observing time necessary to establish the rotation axis of even a bright elliptical galaxy, and so the sample of galaxies sufficiently bright for measurement is quite small and only the weaker radio galaxies can be studied. Nevertheless, the observation of nearby galaxies allows good linear resolution of both the radio and the dynamical features of the galaxies to be achieved, and hence approaches the nuclear properties more closely than does a study of the stellar envelope of a more distant galaxy.

For these reasons, we have chosen to work on an inhomogeneous and incomplete sample of elliptical galaxies which are sufficiently bright to allow good stellar-dynamical mapping. The galaxies used were chosen from all those for which at least one stellar rotation curve was available, and which are listed in Davies *et al.* (1983), Simkin (1979), Jenkins and Scheuer (1980), and Jenkins (1981). Only galaxies at declinations above $-40°$ were included in our sample, to ensure that good radio interferometric maps could be made with the VLA.

III. OPTICAL DATA

The sample of 54 galaxies is listed in Table 1, together with their ellipticities and projected minor axis position angles. Accurate nuclear positions for many of these galaxies have also been measured, and may be obtained from the authors on request. The ellipticities given in Table 1 are taken from Davies *et al.* (1983) and references therein unless otherwise indicated in the notes. Where possible, the position angle of the minor axis in the central regions of the galaxies was taken from published surface photometry. Uncertainties of these values were estimated from the size of the error in individual measurements and the scatter in the quoted values at small radii. For those galaxies with no surface photometry we made our own measurements of position angle to check those tabulated in catalogs of Nilson (1973) and Lauberts *et al.* (1981) and to estimate the error. In most cases our measurements were in good agreement with the catalog values, and the errors tabulated in Table 1 reflect the degree of agreement and the error we attached to our own measurement. The ellipticity and size of the image entered into our internal error estimate, as well as the degree to which the image was confused by stars or dust. A few galaxies were in the approximate declination range $-2°.5$ to $-17°.5$ or were too faint or too round to have entries in the catalogs. In these cases our own measurements are quoted in Table 1. For NGC 1316, 3C 33, and 3C 98 the position angle was taken from individual studies of these galaxies that used photographic material.

There are several difficulties with the measurements of ellipticity and minor-axis position angle that can affect the results, notably, the following.

1. The use of deep plates (e.g., the Palomar Sky Survey plates) to measure the figures of the galaxies assumes that there are no strong isophotal twists between the inner and outer parts of the galaxies. To avoid this assumption we have used

© American Astronomical Society • Provided by the NASA Astrophysics Data System

1985ApJ...291...32B

TABLE 1

GALAXY SAMPLE

Galaxy	Ellipticity	Minor Axis Position Angle (deg)	Notes	Galaxy	Ellipticity	Minor Axis Position Angle (deg)	Notes
NGC 315	0.31	132 ± 3	1	NGC 4374	0.10	44 ± 2	3
3C 33	0.61	163 ± 10	2	NGC 4387	0.38	50 ± 5	7
NGC 584	0.37	147 ± 2	3	NGC 4406	0.24	32 ± 2	3
NGC 596	0.37	12 ± 3	3	NGC 4458	0.05	...	...
NGC 720	0.37	55 ± 2	3	NGC 4472	0.18	70 ± 5	3
NGC 741	0.02	3 ± 5	3	NGC 4473	0.42	40 ± 3	6
NGC 1052	0.31	23 ± 3	4	NGC 4478	0.15	52 ± 6	6
NGC 1316	0.37	150 ± 2	5	NGC 4486	0.14	75 ± 5	4
3C 98	0.30	166 ± 4	2	NGC 4489	0.05	49 ± 12	10
NGC 1600	0.26	98 ± 2	3	NGC 4551	0.19	160 ± 10	7
NGC 1700	0.29	2 ± 3	3	NGC 4621	0.34	70 ± 4	3
NGC 2768	0.56	4 ± 4	6	NGC 4636	0.19	76 ± 5	3
NGC 2778	0.29	130 ± 7	7	NGC 4649	0.19	10 ± 5	3
3C 218	0.08	40 ± 20	8	NGC 4697	0.38	157 ± 5	11
NGC 3377	0.37	134 ± 3	6	NGC 4742	0.34	169 ± 3	3
NGC 3379	0.13	160 ± 3	4	NGC 4839	0.50	152 ± 2	1
NGC 3557	0.32	120 ± 8	9	NGC 4889	0.31	170 ± 10	7
NGC 3605	0.41	107 ± 7	7	IC 4296	0.10	133 ± 10	10
NGC 3608	0.19	168 ± 5	6	NGC 5638	0.09	60 ± 10	7
NGC 3665	0.21	115 ± 3	1	NGC 5813	0.25	42 ± 3	6
NGC 3818	0.32	18 ± 4	10	NGC 5831	0.09	44 ± 6	10
NGC 3904	0.26	98 ± 10	9	NGC 5845	0.35	58 ± 5	3
NGC 3923	0.35	140 ± 10	9	IC 1101	0.33	116 ± 5	1
NGC 3962	0.09	73 ± 6	10	NGC 7562	0.29	172 ± 4	3
NGC 4261	0.17	69 ± 2	3	NGC 7619	0.09	125 ± 3	3
NGC 4278	0.07	130 ± 5	6	NGC 7626	0.17	92 ± 2	3
NGC 4365	0.25	136 ± 2	3	NGC 7785	0.40	45 ± 5	3

NOTES.—(1) Position angle from R. Peletier 1984, private communication. (2) Ellipticity and position angle from Matthews, Morgan, and Schmidt 1964. (3) Position angle from Lauer 1984. (4) Position angle from Davis *et al.* 1984. (5) Position angle and ellipticity from Schweitzer 1980. (6) Position angle from Leach 1981. (7) Position angle from Nilson 1973. (8) Position angle and ellipticity measured from the unpublished CCD data of Heckman. (9) Position angle from Lauberts *et al.* 1981 and references therein. (10) Position angle measured directly from the Palomar Sky Survey or from the ESO Blue Survey for galaxies south of −17°. (11) Position angle from King 1978.

published CCD surface photometry to measure the central minor-axis position angle. Among the 22 galaxies with extended radio structure detected in this study, all but five (3C 33, 3C 98, NGC 1316, NGC 3557, and IC 4296) have position angles determined in this way. Those position angles from Lauer (1984) and R. Peletier (1984, private communication) given in Table 1 were measured at a radius of typically 2″–5″. The position angles taken from Leach (1981) are limited to radii greater than 30″ because of contamination by scattered light at smaller radii. Large isophote twists are unusual, but some do occur; for example, both 3C 33 and NGC 7626 show a 90° twist, and in these cases we have taken the position angle as close to the center as possible. Note that the position angle for NGC 7626 measured by Lauer is 90° different from that given in King (1978).

2. Any undetected dust patches associated with a galaxy will deform its figure and may result in a seriously incorrect measurement of the ellipticity and the minor-axis position angle.

3. For galaxies with low ellipticity, it is intrinsically difficult to measure the location of the minor axis, and hence the position angles of the minor axes of the eight very round galaxies in this sample are quite uncertain.

These uncertainties are, to some extent, reflected in our error estimates, but until surface photometry is available for the five galaxies with position angles determined from sky survey plates, they should be considered as preliminary values.

The ellipticity distribution for our sample of galaxies is shown in Figure 1 (*broken line*), where it is compared with that for elliptical galaxies in de Vaucouleurs, de Vaucouleurs, and Corwin (1976, hereafter RC2), shown as the solid line (see Binney and de Vaucouleurs 1981). It can be seen from the figure that the sample of galaxies *is* somewhat atypical of the general distribution of elliptical galaxies, possessing an excess of flat galaxies. This selection effect is intrinsic to the sample of galaxies previously studied for rotation measurements. Although

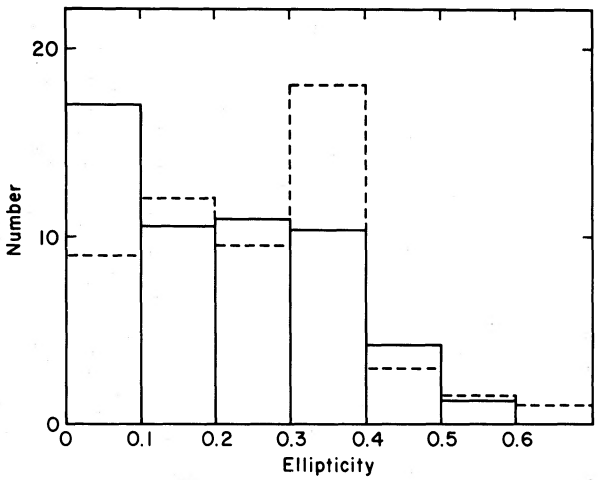

FIG. 1.—The ellipticity distribution in the sample of 54 galaxies (*broken line*) and in the elliptical galaxies in RC2 (*solid line*; derived from Binney and de Vaucouleurs 1981).

© American Astronomical Society • Provided by the NASA Astrophysics Data System

1985ApJ...291...32B

elliptical galaxies have low rotation velocities, on the average flatter galaxies have a higher rotation, so that, in order to detect rotation to a given limit, observers have selected samples of flatter galaxies to obtain more detections of rotation. It seems unlikely that general conclusions concerning the dynamical axes will be affected by this bias, but such a problem is possible.

To derive absolute magnitudes, radio powers, and linear scales from the observed quantities, we have used recession velocities and assumed a uniform Hubble flow with $H_0 = 50$ km s^{-1} Mpc^{-1}. The velocities were taken from Davies *et al.* (1983). For those galaxies not in their compilation the recession velocities were taken from the studies of their rotation curves.

IV. THE RADIO OBSERVATIONS

Of the 54 galaxies listed in Table 1, seven (3C 33, 3C 98, 3C 218, NGC 315, NGC 1052, NGC 4374, and NGC 4486) have excellent maps already published (see Appendix). Radio data on the remaining galaxies are inhomogeneous and incomplete. In order to provide adequate radio information for these objects, all 47 were observed with the Very Large Array (VLA) of the National Radio Astronomy Observatory[2] during 1983 March.

During these observations, the VLA was operated in the C array, with 24–27 antennas in full use at any one time. Observations were made at 4.885 GHz, as a compromise between the detection of central components and of extended structures associated with the galaxies. Data were taken in two 50 MHz wide channels (of opposite circular polarization) simultaneously, and about 10 minutes of integration time was used per source, with the time usually arranged in two 5 minute periods to minimize problems with intermittent interference or faults, and to improve the coverage of the *u-v* plane. The data were phase-calibrated at intervals of about 30 minutes with respect to standard unresolved calibration sources located near the galaxies, and the flux density scale was established by observations of 3C 286 (1328+308) with an assumed 4.885 GHz flux density of 7.41 Jy (Baars *et al.* 1978). The rms noise level achieved in each field was 0.2–0.3 mJy, and the maps presented here are in the *I* Stokes parameter only (strictly, the pseudo-*I*, since visibilities in one channel were used when there was no corresponding visibility in the other channel).

For each field, the visibility data were calibrated, gridded onto the *u-v* plane, and Fourier transformed to produce a high-resolution synthesis map. Flux density limits of three times the noise level at the field center were then established for those fields in which no significant feature was found within a 20″ circle about the nominal position of the galaxy. The visibility data were then checked carefully, to ensure that no detectable low-brightness structures were missed through the construction of the synthesis map (i.e., structures on scales greater than about 60″). Twenty-six galaxies were not detected at this stage, and the flux density limits for small-angular-scale sources located at these galaxies are given in Table 2. The remaining 21 galaxies showed evidence of some radio emission, and their data were further processed. Several unrelated radio sources were also detected, but these are not relevant to this project and will not be discussed further.

If radio emission was apparent in a field, then that field was CLEANed using the standard Astronomical Image Processing System (AIPS) programs available at the VLA site (Clark 1980), and then the CLEAN components removed from the map were restored using a CLEAN beam of Gaussian shape and the same half-width and orientation as the "dirty" beam. For four of the fields (NGC 3379, NGC 3608, NGC 3962, NGC 5813) the sources were too weak for self-calibration of the data (Cornwell 1982) to be useful. For the other sources, the data were self-calibrated, CLEANed again, and corrected for the polar diagram of the VLA primary antennas to produce the final maps. These procedures were not adequate in three cases:

NGC 4478.—The data are somewhat confused by NGC 4486 (which lies ~9′ away). In this case, a map was made centered on NGC 4486, then CLEANed, and the resulting CLEAN components for NGC 4486 then subtracted from the data to produce a residual (i.e., NGC 4486–subtracted) map of NGC 4478. The high noise level at NGC 4478 (Table 2) reflects the extent to which this procedure is inadequate, but represents a hundredfold improvement on the original map.

NGC 4261.—In this case, it was found that the C array of the VLA significantly overresolved the source (with the exception of a central point source, and the narrow jet features; see Appendix). Data at baselines greater than 900 m were therefore removed from the synthesis to produce a low-resolution map of NGC 4261, to show the overall structure of the source. These low-resolution data were then CLEANed and self-calibrated in the same way as the other maps.

NGC 7785.—For this galaxy no point source was detected, and the slight visibility rise at small spacings was not adequately represented on any map. This galaxy was therefore remapped at 408 and 1407 MHz using the Cambridge One Mile radio telescope. The galaxy was detected at both frequencies, with flux densities 92 ± 27 and 18 ± 3 mJy, and an angular size ~20″ (seen as a beam broadening on the 1407

TABLE 2

FLUX DENSITY LIMITS FOR UNDETECTED GALAXIES

Galaxy	4.885 GHz Flux Density Limit at 3 σ (mJy)
NGC 584	1.00
NGC 596	0.95
NGC 720	0.88
NGC 1700	0.64
NGC 2778	0.62
NGC 3377	0.60
NGC 3605	1.15
NGC 3608	0.65
NGC 3818	0.65
NGC 3904	0.92
NGC 3923	0.86
NGC 4365	0.44
NGC 4387	0.53
NGC 4406	0.54
NGC 4458	0.52
NGC 4473	1.18
NGC 4478	1.48
NGC 4489	0.53
NGC 4551	0.50
NGC 4621	0.68
NGC 4697	0.62
NGC 4742	1.00
NGC 5638	0.57
NGC 5831	0.56
NGC 5845	0.63
NGC 7562	0.91

[2] The National Radio Astronomy Observatory is operated by Associated Universities, Inc., under contract with the National Science Foundation.

© American Astronomical Society • Provided by the NASA Astrophysics Data System

1985ApJ...291...32B

MHz map). The 4885 MHz flux density, extrapolated from these data, should be ~3.4 mJy, but no point source stronger than 1.1 mJy could be found in the VLA data.

The locations of point sources in the fields of the galaxies were fitted on the CLEANed maps using the CLEAN beam and the assumption that the underlying source is Gaussian in shape. For six of the sources, only a pointlike component was found, and angular size limits were derived using the fits to the objects and the noise level on the map. In the remaining cases, flux densities for the extended sources were derived from the map by summing the flux density contained in a box around the region containing the source, and checked by inspection of the visibility curves.

Maps of the more extended radio sources are shown in Figures 2*a*–2*k*, and the 21 detected elliptical galaxies are listed in Table 3 together with the seven galaxies that had already been well mapped. Table 3 therefore contains the complete list of galaxies which are available for dynamical studies. It also gives the source power at 4.885 GHz, a classification of the source, the linear size of any jet feature, and the position angle of the radio axis.

The source classifications are generally based on the

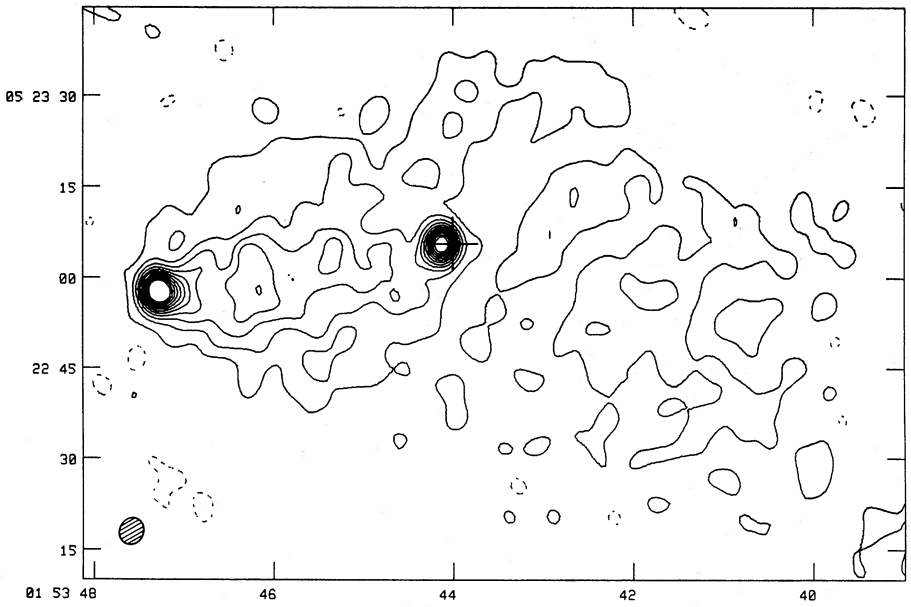

FIG. 2*a*

FIG. 2.—VLA contour maps of the extended radio sources at 4885 MHz in the *I* Stokes parameter. On all maps the location of the galaxy nucleus is marked as a cross, and the synthesized half-power beamwidth is shown as a shaded ellipse. Negative contours are drawn broken. (*a*) NGC 741. Contours are drawn at intervals of 0.8 mJy, starting at −12 mJy. The nucleus of the galaxy NGC 742 is located 2″.0 ± 0″.7 north of the compact region in the eastern lobe.

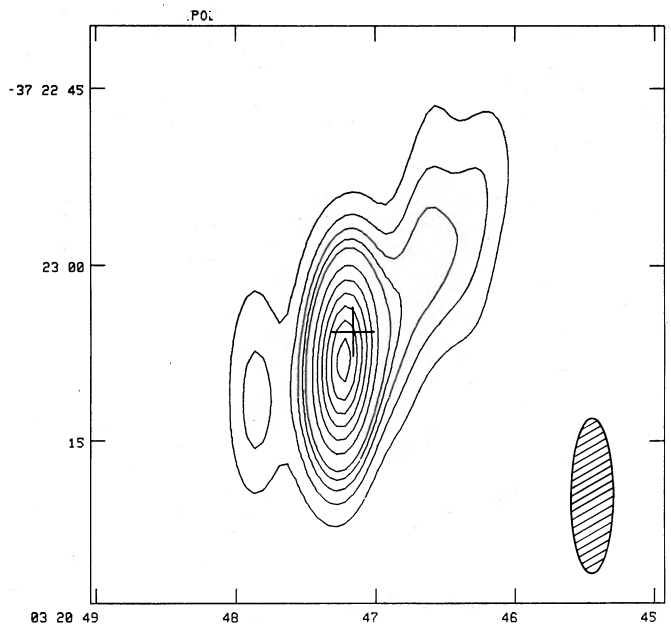

FIG. 2*b*.—NGC 1316. Contours are drawn at intervals of 2 mJy from 2 to 10 mJy, then at 5 mJy intervals.

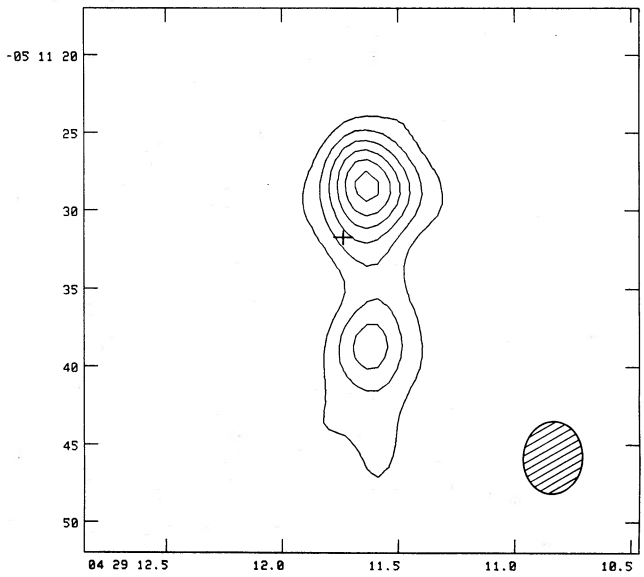

FIG. 2*c*.—NGC 1600. Contours are drawn at 1 mJy intervals from −3 mJy, but without the zero contour.

© American Astronomical Society • Provided by the NASA Astrophysics Data System

1985ApJ...291...32B

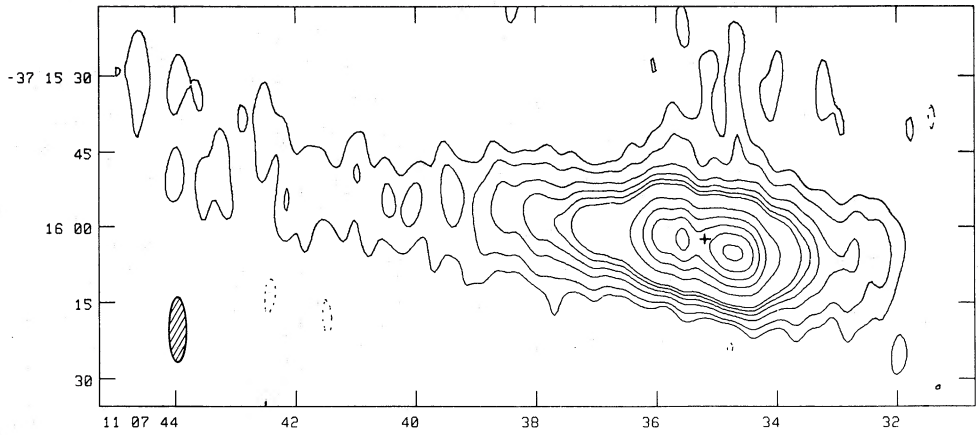

FIG. 2*d*.—NGC 3557. Contours are drawn at −0.5, 0.5, 1, 2, 3, 4, 5, 10, 15, 20, 25, and 30 mJy

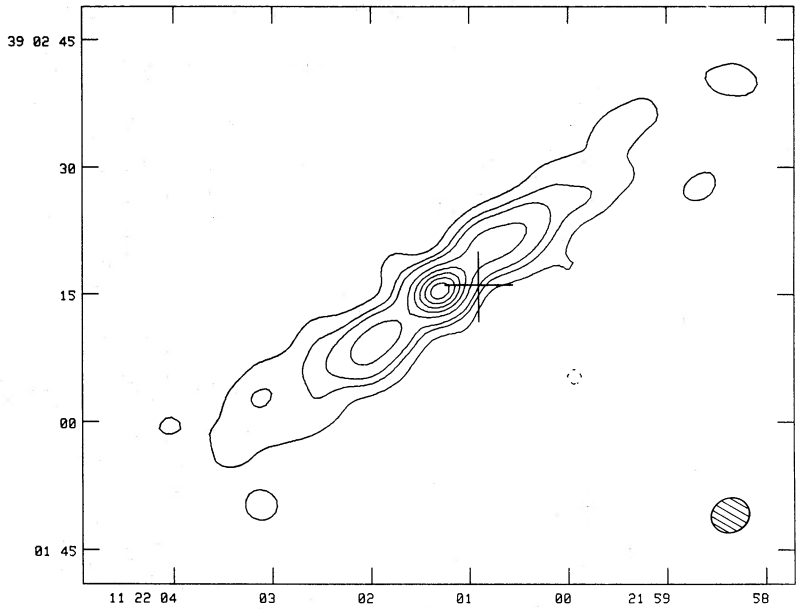

FIG. 2*e*.—NGC 3665. Contours are drawn at −0.4, 0.4, 1.2, 2, 4, 6, 8, 10, and 12 mJy

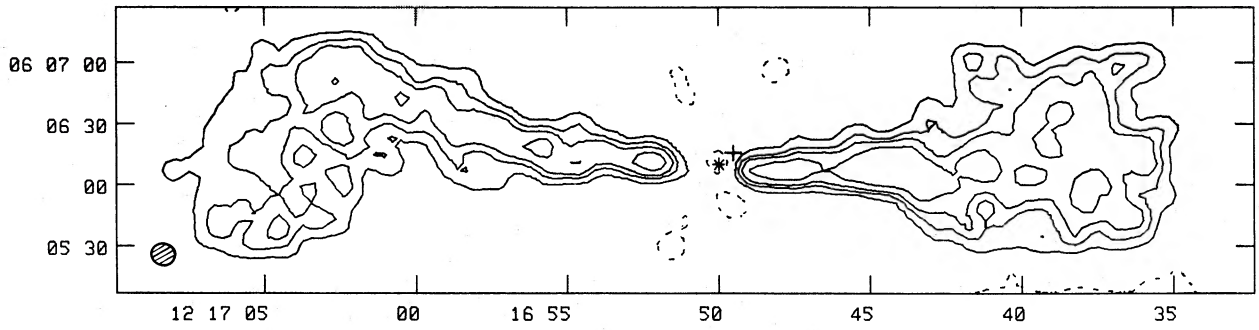

FIG. 2*f*.—NGC 4261. Contours are drawn at −5, 5, 10, 15, and 25 mJy. The asterisk marks the location of a point source of 315 ± 5 mJy that has been subtracted from this map.

© American Astronomical Society • Provided by the NASA Astrophysics Data System

1985ApJ...291...32B

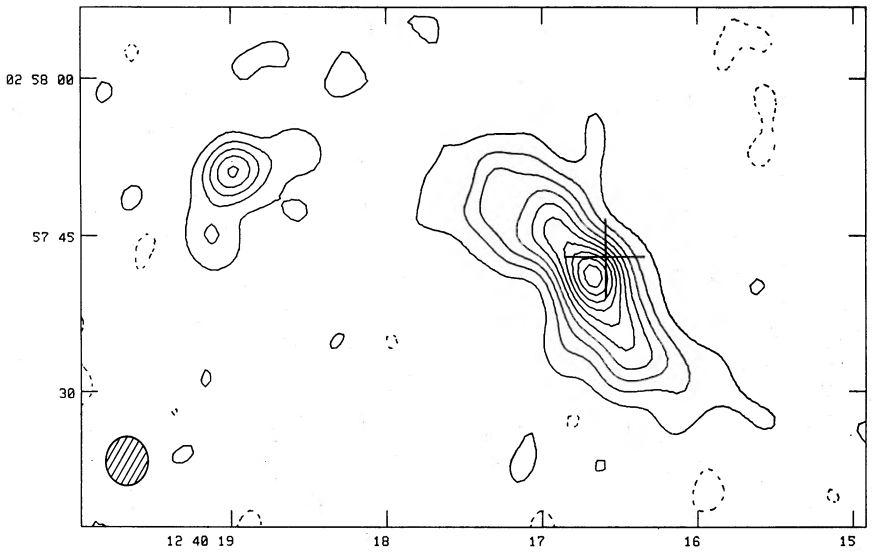

FIG. 2*g*.—NGC 4636. Contours are drawn at intervals of 0.6 mJy, starting at −0.3 mJy

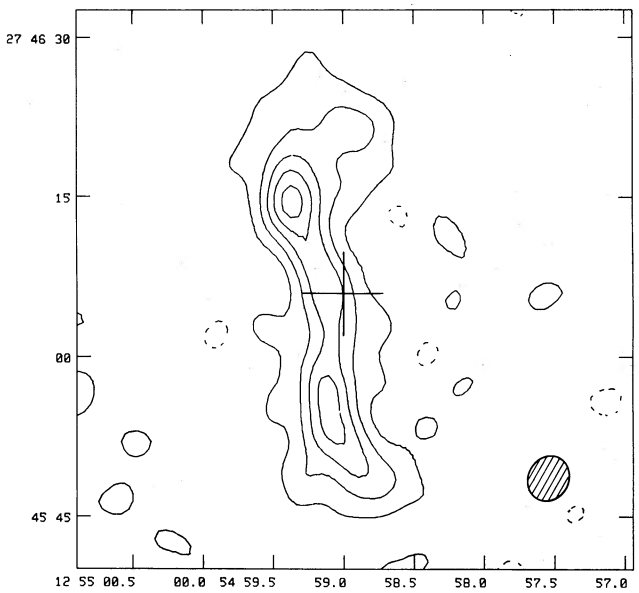

FIG. 2*h*.—NGC 4839. Contours are drawn at intervals of 0.6 mJy, starting at −0.3 mJy.

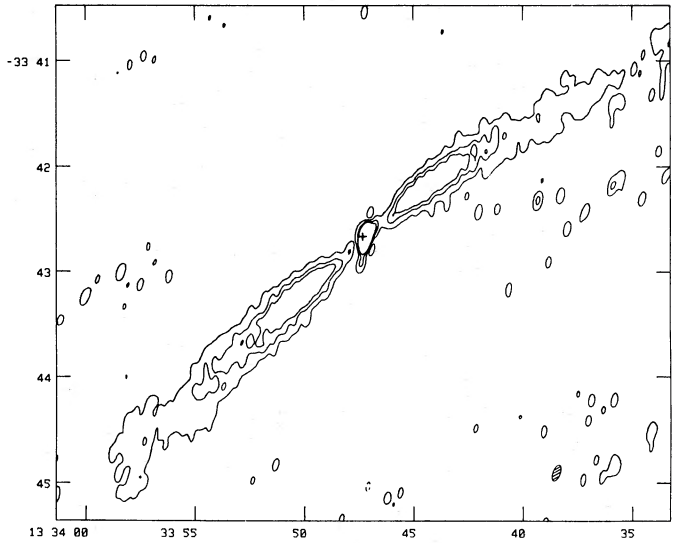

FIG. 2*i*.—IC 4296. Contours are drawn at intervals of 4 mJy, starting at −2 mJy.

observed kpc-scale structures, but in the cases of NGC 1052, NGC 4278, and NGC 4374 the VLBI data were also used. P-type (pointlike) sources are unresolved to the VLA in the C array, and have not been resolved in any other observations. E-type sources are distinguishable only as extended in our VLA data (on the basis of a beam broadening of the source). D-type sources are doubles, either classical, almost symmetrical objects, such as 3C 98, or irregular, such as IC 1101, where there is *no* direct information about the orientation of the beam powering the source. Finally, the J-type sources are those with distinguishable radio jets (such as NGC 4261), where we therefore have direct information of the orientation of a beam, and where we can be relatively confident about the radio axis of the galaxy. Clearly, the J-type sources are those that are preferrred for dynamical study, whereas the P-type, the E-type, and the D-type sources require further, higher resolution radio data to be useful for this purpose. Of the 28 galaxies in Table 3, 15 are of J type.

The radio position angles given in Table 3 are the most useful data from this study. These position angles can be found only on scales larger than the synthesized beam of the telescope: bends in the radio structures on smaller scales will be hidden from our observations. Since it is the *central* radio position angles which are of most importance to our study, it is clear that we must *assume* that there are no striking bends in the structures of the sources on beam-sized scales or smaller. This limitation is implicit for all observations using telescopes with resolution worse than that needed to resolve the beam generator, but it is not likely that this assumption introduces a systematic uncertainty in excess of about 10° in those cases where we see straight jets extending over many beams (e.g., NGC 315, NGC 4261). There is likely to be a larger uncer-

© American Astronomical Society • Provided by the NASA Astrophysics Data System

1985ApJ...291...32B

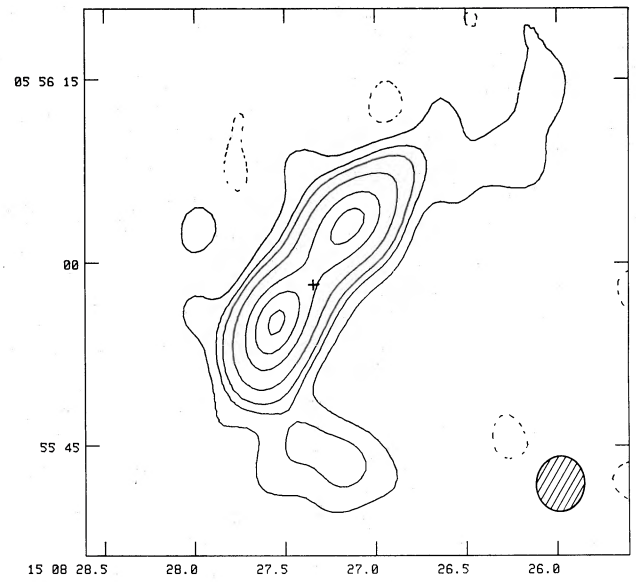

FIG. 2*j*.—IC 1101. Contours are drawn at −0.4, 0.4, 1.2, 2, 2.8, and 3.6 mJy

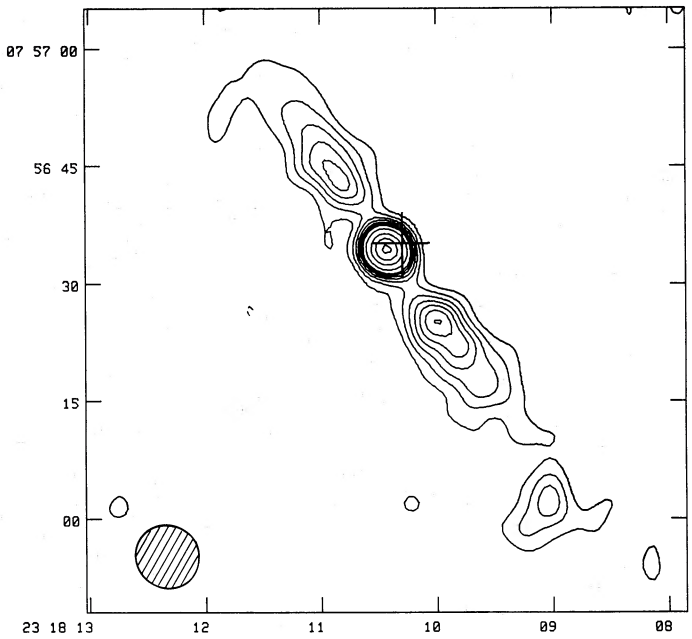

FIG. 2*k*.—NGC 7626. Contours are drawn at −1, 1, 2, 3, 4, 5, 6, 7, 10, 15, 20, 25, and 30 mJy

tainty in cases where the map shows a jet only a few beam sizes long (e.g., NGC 1316) or in cases where no jet is seen (e.g., NGC 1600, IC 1101). Details of the maps and the derivations of these position angles are given in the Appendix, where the sources are discussed individually.

V. DISCUSSION

The primary data obtained from this study are the radio position angles of the sources listed in Table 3. Insufficient dynamical data exist for these objects, at present, for an examination of the alignments of the radio and rotation axes. The relative orientations of the radio and minor axes of the galaxies in this sample are better defined than in earlier work because of the higher linear resolution in both wavebands. A comparison of the radio and minor axes is physically meaningful only if the minor and rotation axes of the galaxies are closely parallel. Davies *et al.* (1983) conclude that this might be the case in many elliptical galaxies, but Jenkins (1982) suggests that a characteristic property of radio-active elliptical galaxies is that the rotation and minor axes are not parallel, so that the stellar figure of a galaxy may give no clue to its underlying dynamics. In addition, there are several difficulties (see § III) with defining the radio and the minor-axis position angles, so that a unique alignment of the radio and minor axes of elliptical galaxies is not to be expected. Nevertheless, several authors have searched for such an alignment, and have concluded that the radio position angles tend to lie close to the minor axes. There have been suggestions (Kapahi and Saikia 1982) that the degree of alignment may depend on the fraction of the flux density of the source appearing in the central component, or that brighter

© American Astronomical Society • Provided by the NASA Astrophysics Data System

1985ApJ...291...32B

TABLE 3

DETECTED GALAXIES

Galaxy	log P_{4885} (W Hz^{-1} sr^{-1})	Source Type	Jet Length (kpc)	Position Angle of Radio Axis (deg)	Notes
NGC 315	23.09	J	400	131 ± 2	1, 2
3C 33	24.85	D	...	19 ± 3	3, 4
NGC 741	22.39	D	...	106 ± 6	1, 5, 6
NGC 1052	21.96	J	1.4×10^{-3}	63 ± 5	1, 7, 8
NGC 1316	21.62	J	32×10^{-3}	126 ± 14	1, 5, 9
3C 98	24.18	D	...	25 ± 5	3, 10
NGC 1600	21.24	D	...	181 ± 15	3, 5
NGC 2768	19.93	P	...	...	1, 5
3C 218	25.17	J	350	24 ± 5	1, 11
NGC 3379	18.31	P	...	...	1, 5
NGC 3557	21.92	J	31	78 ± 6	1, 5
NGC 3665	20.96	J	2 × 6.4	129 ± 3	1, 5
NGC 3962	19.57	P	...	...	1, 5
NGC 4261	22.69	J	2 × 32	88 ± 1	1, 5
NGC 4278	21.18	J	0.6×10^{-3}	152 ± 10	1, 8, 12
NGC 4374	22.02	J	11	2 ± 1	1, 12
NGC 4472	20.46	J	0.3	83 ± 4	1, 6, 13
NGC 4486	23.49	J	3.3	101 ± 1	1, 14
NGC 4636	20.06	J	2 × 1.5	33 ± 8	1, 5
NGC 4649	19.89	P	...	...	1, 5
NGC 4839	21.73	J	2 × 10	10 ± 10	1, 5, 15
NGC 4889	20.23	P	...	...	1, 5
IC 4296	22.96	J	2 × 69	130 ± 2	1, 5
NGC 5813	19.35	P	...	...	1, 5
IC 1101	23.16	D	...	145 ± 10	3, 5
NGC 7619	20.67	E	...	79 ± 42	1, 5
NGC 7626	21.79	J	2 × 15	35 ± 5	1, 5
NGC 7785	20.33	E	...	115 ± 15	3, 5, 16

NOTES.—(1) Compact central component coincides with galaxy nucleus. (2) Radio map in Bridle *et al.* 1979. (3) Radio structure without detected central component overlies nucleus. (4) Radio map in Hargrave and McEllin 1975. (5) This paper; see Appendix and Fig. 2. (6) High-resolution radio map in Laing 1984. (7) VLA map in Wrobel 1984; VLBI map in Jones, Wrobel, and Shaffer 1983. (8) VLBI map in Jones, Wrobel, and Shaffer 1983. (9) Geldzahler and Fomalont 1983. (10) Radio map in Jenkins, Pooley, and Riley 1977. (11) Hydra A: radio map in Ekers and Simkin 1983. (12) VLBI map in Jones, Sramek, and Terzian 1981*a*; VLA map in Jones, Sramek, and Terzian 1981*b*. (13) Large-scale radio map in Ekers and Ekers 1973 and Ekers and Kotanyi 1978. (14) Radio map in Biretta, Owen, and Hardee 1983. (15) Small-scale structure is jetlike but has large extension at low frequencies (see text). (16) Insufficient aperture plane coverage at VLA; these results were derived from lower resolution 408 and 1407 MHz map from the Cambridge One Mile telescope (see Appendix).

sources tend to be better aligned (Palimaka *et al.* 1979). We have too small a sample to allow such a partition of our data to be made, but we may examine the overall distribution of misalignment angles with more certainty because of the higher linear resolution.

The misalignment angles, θ_m (the difference between the radio and projected minor-axis position angles), for each extended source were calculated from the radio position angles given in Table 3 and the minor-axis position angles of Table 1, and are given in Table 4. The distribution of misalignment angles showing the errors is plotted in Figure 3*a* and as a histogram in Figure 3*b*. These diagrams indicate a preference for radio structures to align closer to the minor axis than to the major axis, although some examples of large misalignments are present in the sample. We have been able to study the galaxies in our sample on smaller linear scales than has been possible in earlier work, because they are nearby. We are thus less likely to have been misled by optical or radio morphological peculiarities. The largest uncertainty in all studies of this type relates to whether or not the structure observed on scales of, typically, a kiloparsec is representative of the structure on the smaller scale of the central engine.

We have used the data in Table 4 to estimate the shape of the *underlying* distribution of misalignment angles that these data sample. If we assume that this underlying distribution is characterized by constant probabilities of θ_m in each 10° range, 0°–10°, 10°–20°, ..., 80°–90°, then we may use a Bayesian argument to optimize the probability of obtaining the results in Table 4 with the errors given as a function of the nine probabilities P_{0-10}, P_{10-20}, ..., P_{80-90}. The resulting distribution is shown in Figure 3*c*.

The uncertainties shown in Figure 3*c* emphasize the limitations of the small sample; however, within the range $0° \leq \theta_m < 50°$ the distribution is consistent with being uniform, and larger misalignments are significantly less likely. If the radio and minor axes were independent, then we would expect the

© American Astronomical Society • Provided by the NASA Astrophysics Data System

1985ApJ...291...32B

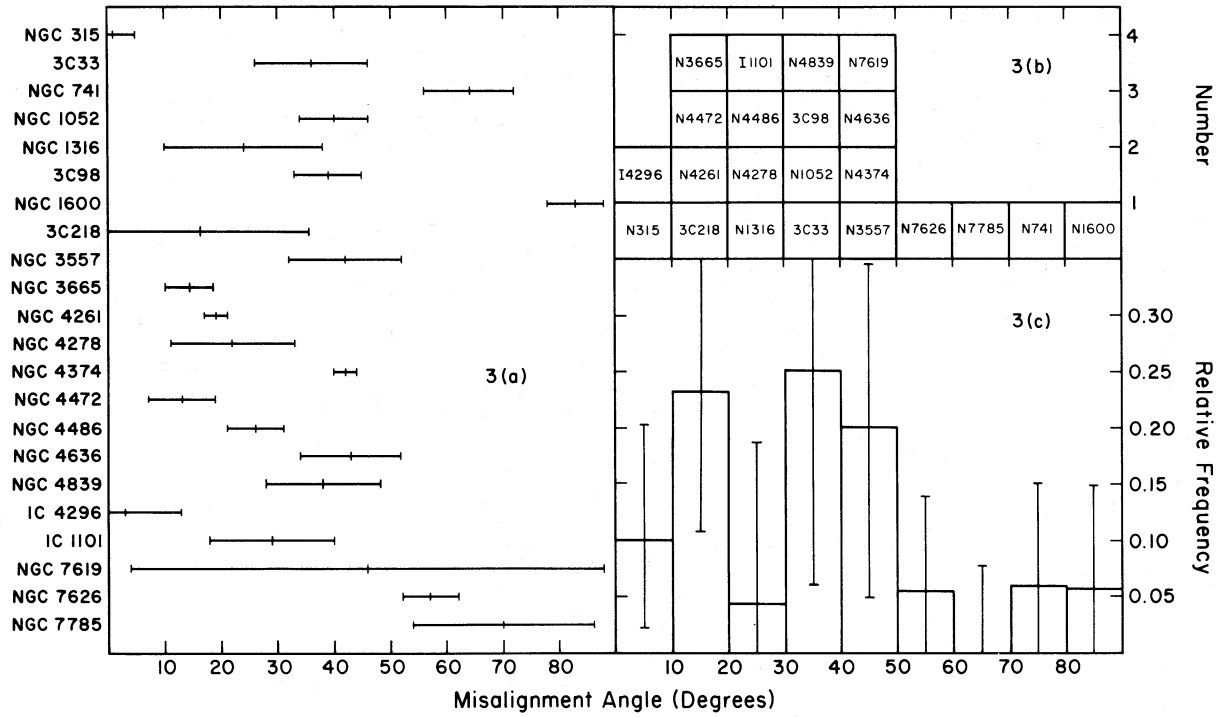

FIG. 3.—The misalignment angles between the radio emission and minor axes. (*a*) The misalignment angle and error for each extended radio galaxy in the sample. (*b*) The distribution of misalignments, drawn on a histogram with 10° bins. (*c*) The calculated underlying probability distribution with $\pm 1\ \sigma$ error bounds in each 10° bin. See text for details of the calculation.

distribution of misalignment angles to be uniform between 0° and 90°. This is not consistent with the data at the 95% confidence level. The probability of the misalignment angle being in the range 0°–50° is 0.83 ± 0.08. These results are not changed significantly if we exclude those galaxies without CCD surface photometry.

In making the above comparison, we have assumed that the figures of the galaxies under study are oblate or, if triaxial, then close to oblate. Only if these galaxies have oblate figures is the projected minor axis coincident with the minor axis of the 3D figure, so that the comparison of the projected minor axis with that of the radio axis is physically reasonable. Davies *et al.* (1983) found that the lower luminosity elliptical galaxies are likely to be oblate, and the differential rotation implied by the flat rotation curves of many brighter elliptical galaxies suggests that they are unlikely to be prolate.

In Figure 4 the ellipticity distribution of the detected galaxies (*dashed line*) is compared with that for the full sample (*full line*). It can be seen that there is no significant difference, so that for this sample there is no strong dependence of radio

TABLE 4

RADIO AXIS AND OPTICAL MINOR AXIS ALIGNMENTS

Galaxy	Position Angle of Radio Axis	Position Angle of Galaxy Minor Axis	Misalignment Angle
NGC 315	131 ± 2	132 ± 3	−1 ± 4
3C 33	19 ± 3	163 ± 10	36 ± 10
NGC 741	106 ± 6	3 ± 5	−77 ± 8
NGC 1052	63 ± 5	23 ± 3	40 ± 6
NGC 1316	126 ± 14	150 ± 2	−24 ± 14
3C 98	25 ± 5	166 ± 4	39 ± 6
NGC 1600	181 ± 15	98 ± 2	83 ± 15
3C 218	24 ± 5	40 ± 20	−16 ± 20
NGC 3557	78 ± 6	120 ± 8	−42 ± 10
NGC 3665	129 ± 3	115 ± 3	14 ± 4
NGC 4261	88 ± 1	69 ± 2	19 ± 2
NGC 4278	152 ± 10	130 ± 5	22 ± 11
NGC 4374	2 ± 1	44 ± 2	−42 ± 2
NGC 4472	83 ± 4	70 ± 5	13 ± 6
NGC 4486	101 ± 1	75 ± 5	26 ± 5
NGC 4636	33 ± 8	76 ± 5	−43 ± 9
NGC 4839	10 ± 10	152 ± 2	38 ± 10
IC 4296	130 ± 2	133 ± 10	−3 ± 10
IC 1101	145 ± 10	116 ± 5	29 ± 11
NGC 7619	79 ± 42	125 ± 3	−46 ± 42
NGC 7626	35 ± 5	92 ± 2	−57 ± 5
NGC 7785	115 ± 15	45 ± 5	70 ± 16

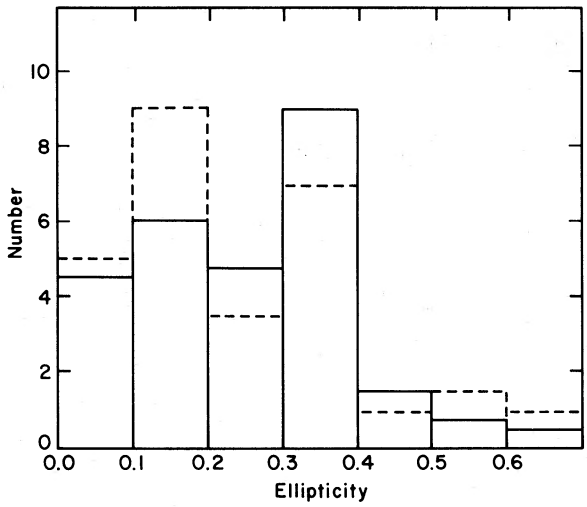

FIG. 4.—The ellipticity distribution in the detected galaxies from our sample (*broken lines*) and in the sample as a whole, on the assumption that the detection probability is independent of ellipticity (*solid lines*).

© American Astronomical Society • Provided by the NASA Astrophysics Data System

1985ApJ...291...32B

properties on ellipticity. However, this sample is too inhomogeneous to contradict the conclusion of Hummel, Kotanyi, and Ekers (1983) that round galaxies are more likely to be radio sources.

We have searched for correlations between the radio and kinematic properties of those galaxies in common with the sample of Davies *et al.* (1983). If material intrinsic to the host galaxy fuels the radio source, we might expect that fuel from galaxies with faster rotations would exert a larger torque on the central object and therefore, on the average, have smaller misalignment angles. No significant correlation of this type is present in this sample. Further, no significant correlation was found between misalignment angle and ellipticity, absolute magnitude, or the ratio of rotation velocity to velocity dispersion, v/σ. We do find a weak correlation between absolute magnitude and radio power at 4885 MHz. No significant correlation between radio power and rotation velocity, ellipticity, v/σ, misalignment angle, or central velocity dispersion is present in these data. The absence of a correlation between radio power and central velocity dispersion suggests that the presence of a radio source in a galaxy is not related to its ability to retain gas in its central regions.

If the interstellar material that acts as fuel is only recently accreted to the galaxy (extrinsic fuel supply), then the radio and stellar axes may be strongly misaligned. This would suggest that those galaxies with larger misalignment angles should show more dust and gas than the more nearly aligned galaxies. Although this idea is supported by the presence of much dust and ionized gas in NGC 1052, there are insufficient data for most of the sample.

VI. CONCLUSIONS

We present synthesis observations of 47 elliptical galaxies made with the VLA. Together with the seven existing maps, these galaxies form a sample for the investigation of the radio and kinematic properties of elliptical galaxies. Of the 54 galaxies in the sample, 22 show extended structure. We find the following:

1. The distribution of misalignment angles is consistent with being uniform between 0° and 50°, with larger misalignments having a significantly lower frequency. There is an 83% probability of the misalignment angle for a given galaxy being between 0° and 50°.
2. There is a weak tendency for optically luminous galaxies to possess more powerful radio sources.
3. There are no significant correlations between the radio and kinematic properties of the galaxies in this sample, in particular between misalignment angle and rotation velocity or between central velocity dispersion and radio power.

The only connections we find between the radio and optical properties of this sample of galaxies are the preference for smaller rather than larger misalignment angles and the weak correlation between optical and radio luminosity. This is not strong support for the hypothesis that the galaxies that host radio galaxies are intrinsically different from those that do not. Investigation of the orientations of the rotation axes of these galaxies will provide a clearer test of that hypothesis.

We wish to thank the director and staff of the VLA for an allocation of telescope time and for assistance in collecting and calibrating the data. We are grateful to Reynier Peletier and Tim Heckman for access to unpublished data. We thank the directors of the Institute of Astronomy, Cambridge, England, where the positions and position angles of the galaxies were measured from paper copies of the Palomar Observatory Sky Survey. M. B. thanks Gonville and Caius College, Cambridge, for a research fellowship, and the UK Science and Engineering Research Council and the Royal Society for travel support.

APPENDIX

NGC 315 (B2.2 0055+30).—The radio structure of this source is discussed by Bridle *et al.* (1984) but is already adequately represented on the lower resolution map of Bridle *et al.* (1979). The source shows a prominent radio jet extending ~400 kpc to the northwest of a strong central component, a fainter counterjet to the southwest, and diffuse lobes of radio emission to northwest and southeast. Since the radio jet shows no large bends in the first ~2′ of its length, the radio position angle is reliable and well determined.

3C 33 (A0106+13).—This source is a "classical" double (Hargrave and McEllin 1975), with diffuse lobes and compact hot spots, well aligned through a strong central component. No radio jet has been detected in this source, so that the radio position angle given in Table 3 assumes that the beam runs without bends from the nucleus to either hot spot. The uncertainty in the position angle reflects only the widths of the hot spots, and the slight misalignment between them and the central component.

NGC 741.—This source has previously been mapped at 2.7 GHz by Jenkins and Scheuer (1980), at lower N-S resolution than our map, shown in Figure 2*a*. The source shows a compact nucleus associated with NGC 741, a compact eastern hot spot, and a diffuse western component. The eastern component is connected with the nucleus through a bright ridge of emission that might be a diffuse jet. The source is classified as of D type, since no well-defined jet is seen in our data, although the position angle of the bright ridge (100° ± 5°) can be measured accurately. At higher resolution, Laing (1984) finds the nucleus to be significantly extended in position angle 112° ± 5°; the position angle reported in Table 3 is, therefore, the average of the ridge and central radio position angles, or 106° ± 6°, significantly different from the position angle given by Jenkins and Scheuer (1980). Note that the eastern hot spot lies 2.″0 ± 0.″7 south of the nucleus of NGC 742. The structure of the radio source suggests that this is a chance coincidence.

NGC 1052.—The radio position angle for this object, 63° ± 5°, was taken as the average of the direction of the ~10 milli-arsec jet on the VLBI map of Jones, Wrobel, and Shaffer (1983) and the direction from the nucleus to the bright, unresolved knot to the northeast, seen on the VLA map of Wrobel (1984). This direction is opposite to that of the weak ridge of emission to the southwest of the nucleus on Wrobel's map. The source is predominantly double in structure on scales accessible to the VLA, but is jetlike to the VLBI, and hence is classified here as of J type.

NGC 1316.—(Fornax A; see Fig. 2*b*).—The large-scale structure of this source is well known (e.g., Cameron 1971) to consist of two large lobes to either side of a bright central component. Our map overresolves the outer structure, and displays only the inner structure of the source. The extensions to the north-

© American Astronomical Society • Provided by the NASA Astrophysics Data System

1985ApJ...291...32B

west and southeast of the nucleus are seen to be significantly misaligned: a higher resolution map of the nucleus of NGC 1316 (Geldzahler and Fomalont 1983) exhibits an inner double-sided jet structure and shows that this misalignment persists to smaller angular scales. Allowing for this misalignment in the assignment of errors, we classify the source as of J type, and the position angle in Table 3 is the mean position angle of the two sides of the jet.

3C 98.—(A0356+10; see Jenkins, Pooley, and Riley 1977).—This double source has prominent hot spots embedded in diffuse lobes sited symmetrically to either side of the central galaxy, but with the hot spots significantly misaligned with a line through the galaxy. The position angle is derived as the mean position angle of the hot spots with respect to the galaxy, plus or minus half the difference.

NGC 1600 (Fig. 2*c*).—The morphology of this source is clearly double, with the galaxy lying closer to the brighter northern component. Higher resolution radio observations are needed to determine the position angle of any radio jet: the estimate of error in the position angle of the radio axis in Table 3 is derived from the widths of the radio lobes.

NGC 2768.—This weak source is unresolved in our observations.

3C 218 (A0915−11; Hydra A).—This source has a structure of the core-halo type on large angular scales, but has a short embedded jet in position angle 24° ± 5° when examined at higher resolution (Ekers and Simkin 1983). Unpublished direct CCD data on 3C 218 was kindly provided by Heckman and was analyzed using the GASP package at Kitt Peak (Davis *et al.* 1984). We found a large change in position angle of the minor axis from 100° at $r = 2''$ to 150° at $r = 8''$. This measurement may be inaccurate because the galaxy is small and almost round, and there is an interfering image 9″ to the southeast of the galaxy center.

NGC 3379.—This source is barely detected in our data, and is unresolved.

NGC 3557 (see Fig. 2*d*).—This double-sided source displays a prominent knot to the southwest of the galaxy nucleus, and a long radio jet to the northeast. The structures of the two sides of the source are well aligned, and the position angle of the jet is well determined.

NGC 3665 (B2.2 1122+39; Fig. 2*e*).—A 2.7 GHz map of this source is given by Jenkins (1982). Our data resolve the source well into a two-sided jetlike structure, with a prominent central component associated with the nucleus of the galaxy. The position angle of the radio structure is well determined from this map.

NGC 3962.—This source is unresolved in our data.

NGC 4261 (3C 270; Fig. 2*f*).—This map, from which a strong (315 ± 5 mJy) central component at the location of the galaxy nucleus has been removed, shows the overall structure of the source deduced from the short-baseline data. The longer baseline data show the nuclear source to be unresolved, and the jets to be straight with an opening angle of less than 5° out to 30″ from the nucleus. The jets are aligned to within 1° in this region, and the small error quoted for the radio position angle in Table 3 reflects this structure.

NGC 4278.—Although this source is unresolved in our data, VLBI observations (Jones, Wrobel, and Shaffer 1983) show it to possess a ∼6 milli-arcsec extension in position angle −28° ± 10°. On the basis of these data, the structure is tentatively classified as jetlike in Table 3.

NGC 4374 (3C 272.1).—The arcsec- and milli-arcsec-scale structures of this source have been reported by Jones, Sramek, and Terzian (1981*a*, *b*) and show a jetlike structure which twists by less than about 1° between its inner (pc-scale) and outer (kpc-scale) regions.

NGC 4472.—Observations of this source by Ekers and Ekers (1973) and Ekers and Kotanyi (1978) have shown it to be a ∼150″ E-W double. Our map shows only a ∼3.″3 beam broadening in position angle 78° ± 6°, consistent with the higher resolution map of Laing (1984), which shows the core to contain well-defined ∼3″ "jet" structure with the jets lying in position angle 83° ± 4°. The source is classified as of J type in its inner structure in Table 3.

NGC 4486 (3C 274; Virgo A).—This source has been mapped often and well in the radio (e.g., Biretta, Owen, and Hardee 1983) and has a prominent radio and optical jet in position angle 280.°5 ± 0.°5, with low surface brightness lobes to east and west of the nucleus.

NGC 4636 (Fig. 2*g*).—This source is the strongest in a field containing five sources. Its form is jetlike, with a strong ridge of radio emission lying to either side of the nucleus of the galaxy. The ridge is resolved both transverse to its length and along it, and shows S-shaped bends ∼5 kpc from the nucleus. The adjacent radio source (at R.A. $12^h40^m19^s.0$, decl. +02°57′51.″2) is unidentified, and may be associated with the main radio structure of the galaxy.

NGC 4839 (Fig. 2*h*).—In our map this source is well resolved along its major axis, which is at position angle 10° ± 10°. The brightness of the ridge is enhanced at the location of the galaxy nucleus, suggesting the presence of a central component of about 0.5 mJy. A 2.7 GHz map of this source is given by Jenkins (1982) and shows similar features. At 151 MHz, however, the source is found to possess a large (∼6′) extension of low surface brightness to the southwest (Cordey 1984), suggesting that much low-brightness structure has been resolved out in our map.

NGC 4649.—This source appears pointlike in our data.

NGC 4889.—This is the weakest source detected in our survey and appears unresolved.

IC 4296 (Fig. 2*i*; PKS 1333−33).—Low-resolution maps of this source are given by Schilizzi and McAdam (1975) and Goss *et al.* (1977), and show an object ∼40′ in overall size, with a bright ridge to either side of the galaxy ending in diffuse faint regions. Our map shows only the inner 5′ of the source, where the ridge of Goss *et al.* is resolved into a thin, symmetrical jet lying to either side of a strong central component associated with the galactic nucleus. The jet shows only slight bends over its inner 10 kpc and has a well-defined position angle.

NGC 5813.—This weak source is unresolved in our map.

IC 1101 (Fig. 2*j*).—This object is the central cD galaxy in Abell 2029, and was mapped at Bonn by Andernach, Waldthausen, and Wielebinski (1978). The single-dish flux density for this source exceeds the maximum flux density on small spacings found by the VLA, and suggests that there is some low-brightness emission lost from our synthesis. The map shows a nearly symmetrical double source disposed to either side of the galaxy nucleus, and the radio position angle of any jet or beam is intrinsically uncertain (Table 3).

NGC 7619.—This source is barely resolved by our observation, and the position angle of the extension is not well determined.

NGC 7626 (Fig. 2*k*).—This source has previously been mapped at 2.7 GHz by Jenkins (1982); our data given an improved determination of the position angle of the radio

© American Astronomical Society • Provided by the NASA Astrophysics Data System

1985ApJ...291...32B

structure. The structure of the source is that of a well-defined jet, rather similar to IC 4296, and again the full extent of the source is probably not represented on this map; there is likely to be substantial missing flux density.

To summarize, of the 28 sources in Table 3, six are pointlike (P), two are extended (E), five are double-structured (D), and the remaining 15 are jetlike (J), with relatively well-determined radio position angles, and are suitable for dynamical mapping.

REFERENCES

Andernach, H., Waldthausen, H., and Wielebinski, R. 1978, *Astr. Ap. Suppl.*, **41**, 339.
Baars, J. W. M., Genzel, R., Pauliny-Toth, I. I. K., and Witzel, A. 1977, *Astr. Ap.*, **61**, 99.
Binney, J. 1978, *M.N.R.A.S.*, **183**, 501.
Binney, J., and de Vaucouleurs, G. 1981, *M.N.R.A.S.*, **194**, 679.
Biretta, J. A., Owen, F. N., and Hardee, P. E. 1983, *Ap. J. (Letters)*, **274**, L27.
Blandford, R. D., and Rees, M. J. 1974, *M.N.R.A.S.*, **169**, 395.
Bridle, A. H., Davis, M. M., Fomalont, E. B., and Willis, A. G. 1979, *Ap. J. (Letters)*, **228**, L9.
Bridle, A. H., Palimaka, J. J., Fomalont, E. B., and Henriksen, R. N. 1984, in press.
Burch, S. F. 1977, *M.N.R.A.S.*, **181**, 599.
Burns, J. O., and Christiansen, W. A. 1980, *Nature*, **287**, 208.
Cameron, M. J. 1971, *M.N.R.A.S.*, **152**, 439.
Clark, B. 1980, *Astr. Ap.*, **89**, 355.
Cordey, R. 1984, private communication.
Cornwell, T. 1982, in *Proc. NRAO–VLA Workshop 5, Synthesis Mapping*, ed. A. R. Thompson and L. R. D'Addario (Green Bank: NRAO), chap. 13.
Davies, R. L., Efstathiou, G., Fall, S. M., Illingworth, G., and Schechter, P. L. 1983, *Ap. J.*, **266**, 41.
Davies, R. L., and Illingworth, G. 1985, preprint.
Davis, L., Cawson, M., Davies, R. L., and Illingworth, G. D. 1984, preprint.
de Vaucouleurs, G., de Vaucouleurs, A., and Corwin, H. G., Jr. 1976, *Second Reference Catalogue of Bright Galaxies* (Austin: University of Texas Press). (RC2)
Ekers, R. D., and Ekers, J. A. 1973, *Astr. Ap.*, **24**, 247.
Ekers, R. D., and Kotanyi, C. E. 1978, *Astr. Ap.*, **67**, 47.
Ekers, R. D., and Simkin, S. M. 1983, *Ap. J.*, **265**, 85.
Geldzahler, B. J., and Fomalont, E. B. 1983, private communication.
Goss, W. M., Wellington, K. J., Christiansen, W. N., Lockhart, I. A., Watkinson, A., Frater, R. H., and Little, A. G. 1977, *M.N.R.A.S.*, **178**, 525.
Guthrie, B. N. G. 1979, *M.N.R.A.S.*, **187**, 581.
Hargrave, P. J., and McEllin, M. 1975, *M.N.R.A.S.*, **173**, 37.
Hummel, E., Kotanyi, C. G., and Ekers, R. D. 1983, *Astr. Ap.*, **127**, 205.
Illingworth, G. 1977, *Ap. J. (Letters)*, **218**, L43.
Jenkins, C. J., Pooley, G. G., and Riley, J. M. 1977, *Mem. R.A.S.*, **84**, 61.
Jenkins, C. R. 1981, *M.N.R.A.S.*, **196**, 987.
———. 1982, *M.N.R.A.S.*, **200**, 705.
Jenkins, C. R., and Scheuer, P. A. G. 1980, *M.N.R.A.S.*, **192**, 595.
Jones, D. L., Sramek, R. A., and Terzian, Y. 1981*a*, *Ap. J.*, **246**, 28.
———. 1981*b*, *Ap. J. (Letters)*, **247**, L57.
Jones, D. L., Wrobel, J. M., and Shaffer, D. B. 1983, *Ap. J.*, **276**, 480.
Kaphai, V. K., and Saikia, D. J. 1982, *J. Ap. Astr.*, **3**, 161.
King, I. R. 1978, *Ap. J.*, **222**, 1.
Laing, R. A. 1984, private communication.
Lauberts, A., Holmberg, B., Schuster, H. E., and West, R. M. 1981, *Astr. Ap. Suppl.*, **46**, 311.
Lauer, T. R. 1984, preprint.
Leach, R. 1981, *Ap. J.*, **248**, 485.
Matthews, T. A., Morgan, W. W., and Schmidt, M. 1964, *Ap. J.*, **140**, 35.
Nilson, P. 1973, *Uppsala General Catalogue of Galaxies* (*Uppsala Astr. Obs. Ann., Vol.* **6**).
Palimaka, J. J., Bridle, A. H., Fomalont, E. B., and Brandie, G. W. 1979, *Ap. J. (Letters)*, **231**, L7.
Perley, R. A., Dreher, J. W., and Cowan, J. J. 1984, *Ap. J. (Letters)*, **285**, L35.
Readhead, A. C. S., Cohen, M. H., and Blandford, R. D. 1978, *Nature*, **272**, 131.
Rees, M. J. 1978, *Nature*, **275**, 516.
Saunders, R., Baldwin, J. E., Pooley, G. G., and Warner, P. J. 1981, *M.N.R.A.S.*, **197**, 287.
Schechter, P. L., and Gunn, J. E. 1979, *Ap. J.*, **229**, 472.
Schilizzi, R. T., and McAdam, W. B. 1975, *Mem. R.A.S.*, **79**, 1.
Schweitzer, F. 1980, *Ap. J.*, **237**, 303.
Simkin, S. 1979, *Ap. J.*, **234**, 56.
Williams, T. B. 1981, *Ap. J.*, **244**, 458.
Wrobel, J. M. 1984, preprint.

M. BIRKINSHAW: Department of Astronomy, Harvard University, 60 Garden Street, Cambridge, MA 02138

R. L. DAVIES: Kitt Peak National Observatory, National Optical Astronomy Observatories, P.O. Box 26732, Tucson, AZ 85726-6732

© American Astronomical Society • Provided by the NASA Astrophysics Data System